Optik 154 (2018) 286–293

Optik

journal homepage: www.elsevier.de/ijleo

Full length article

Investigation of structural, optical and electrical properties of ZnS thin films prepared by ultrasonic spray technique for photovoltaic applications

A. Derbali [a], A. Attaf [a,*], H. Saidi [a], H. Benamra [a], M. Nouadji [a], M.S. Aida [b], N. Attaf [c], H. Ezzaouia [d]

[a] Laboratory of Thin Films and Applications LPCMA, University of Biskra, Algeria, BP 145 RP, 07000 Biskra, Algeria
[b] Departement of Physics Faculty of Sciences, King Abdulaziz University, Djeddah, KSA, Saudi Arabia
[c] Laboratoire de Couches Minces et Interfaces Faculté des Sciences Université de Constantine, Algeria
[d] Laboratoire des Semi-Conducteurs, Nanostructures et Technologie Avancée, Research and Technology Centre of Energy, Borj-Cedria Science and Technology Park, BP 95, 2050 Hammam-Lif, Tunisia

ARTICLE INFO

Article history:
Received 25 March 2017
Received in revised form
26 September 2017
Accepted 6 October 2017

Keywords:
Zinc sulphide
Thin films
Ultrasonic spray
Deposition time
XRD
Optical and electrical properties

ABSTRACT

ZnS films have important applications in photovoltaic devices. In the current study, the ZnS films were deposited by ultrasonic spray method on heated glass substrate at temperature equal to 450 °C.

In this article, we report the effect of deposition time on the different structural, optical and electrical properties of ZnS. All the samples obtained were treated using X-ray diffraction (XRD), optical transmittance spectroscopy (UV-V) and four-point method. The results of X-rays diffraction showed that the deposited material was pure zinc sulfide having a cubic sphalerite structure with preferential orientation along the (111) direction. As well the grain size was around 38–102 nm, when the deposition time increases. The transmittance measurements exhibit an average optical transparency between 35 and 75% in the visible range (400–750 nm) for different deposition times. The direct band gap energy for all films was calculated and found to be from 3.48 to 3.92 eV. The films' thickness is increased with deposition time from 195 nm to 1756 nm. The electric resistivity of the deposited film varies also with the deposition time between 1.51×10^5 and 20.84×10^5 Ω.cm.

1. Introduction

ZnS compound is one of the most important semiconductor material, and it has been largely investigated in the recent years [1]. Due to the wide band gap (3.7 eV), non toxicity, safety to environment and high transparency [2] of ZnS, it can be useful for extensively applications in optoelectronic devices, such as light-emitting diode and laser diode from blue to ultraviolet band [3], fluorescence and electroluminescence thin film devices [4] and n-type window material in solar cell [5]. As well in comparison with CdS, the ZnS thin films are present better lattice matching to CIGS owing to the precedent advantages.

* Corresponding author.
E-mail address: ab.attaf@gmail.com (A. Attaf).

https://doi.org/10.1016/j.ijleo.2017.10.034
0030-4026/

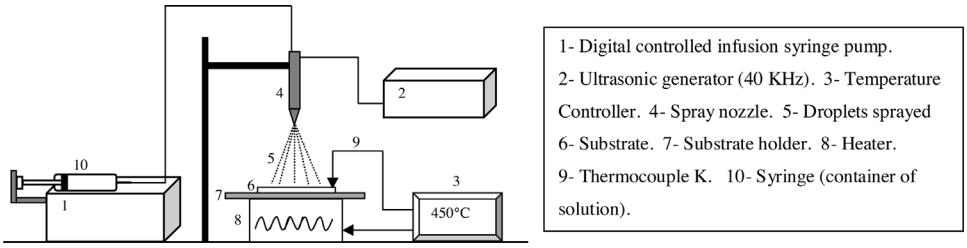

Fig. 1. The schematic experimental to used of deposition system.

Table 1
The deposition condition used to deposited of ZnS thin film.

Deposition condition	Corresponding values
Amount of solution	30 ml
Substrate – nozzle distance	50 mm
Substrate temperature	450 °C
Molarity of solution	0.1M
Deposition time	2 min, 4 min, 6 min, 8 min, 10 min
Spraying flow rate	50 ml/h

According to the literature, Zinc sulphide films can be deposit by several methods including reactive sputtering [6], electro-deposition [7], pulsed-laser deposition [8], chemical vapor deposition (CVD) [9], molecular beam epitaxy (MBE) [10], spray pyrolysis [11], chemical bath deposition (CBD) [12] and sol-gel process [13]. Among those methods, ultrasonic spray is the best one suited for the preparation of Zinc sulphide (ZnS) thin films because it is simplicity and do not cost an experimental requirement, ease of adding various doping materials, reproducibility, speed growth rate and mass production capability for uniform large area coatings [14].

In this paper, we attended zinc sulphide (ZnS) thin films on the glass substrate by ultrasonic spray technique. The aim of this work is to investigate the structural, electrical and optical properties of ZnS films as a function of deposition time. The obtained results are discussed and compared with other research results reported in the literature.

2. Experimental details

The deposition system has been prepared in the laboratory by the simple setup showed in (Fig. 1). Zinc sulphide thin films were deposited on glass substrates of the dimension (25×15) mm^2 using spray ultrasonic technique. These ZnS thin films exhibited good adherence to the substrate surfaces. The glass substrates were cleaned in acetone, ethanol, and distilled water respectively for 15 min, and then blowing dry with a compressed air. The starting solution was prepared by dissolving 0.1 M of Zinc Chloride ($ZnCl_2$) and thiourea ($SC(NH_2)_2$) in methanol. All the parameters were kept constant such as: the substrate temperature (450 °C), the flow rate solution (50 ml/h), the distance nozzle-substrate (50 mm). While, the deposition time changed from 2, 4, 6, 8, 10 min. In the Table 1, we summarized all the deposition condition.

Commonly when the solution droplets reach to the heated substrate surface, the following chemical reaction occurs:

$$ZnCl_2 + CS(NH_2)_2 + CH_3OH + \frac{3}{2}O_2 \rightarrow ZnS + 2NH_4Cl\,(gas) + 2CO_2\,(gas)$$

According to this reaction, a ZnS thin film should be formed on the glass substrate surface and the NH_4Cl, CO_2 leaves the system in gases form.

The structural, optical and electrical characteristics of these films have been studied extensively through several techniques. For the crystalline structure properties of the film was analyzed using X-ray diffracto-meter (D8 ADVANCED BRUKER) with Cu-Kα radiation (λ = 1.5418 Å) in 2θ range from 10° – 90°.

The optical properties have been recorded by using an ultraviolet-visible (UV-VIS) spectrophotometer (PerkinElmer LAMBDA25) between the wavelengths of 300 and 1100 nm. Moreover the electrical resistivity was determined using the four-point method at room temperature.

3. Results and discussion

3.1. Structural properties

According to the deposition process and experimental factors, Zinc sulphide films can be crystallized in two forms, cubic (Zinc blend) and hexagonal. The Fig. 2 shows XRD patterns of ZnS thin films deposited by ultrasonic spray at different deposition times. It was observed at different deposition time that there is a single one peak for all films with the preferred oriented growth along (111) plane at the diffraction angles of 28.7° and this is compatible with exhibited a zinc blende

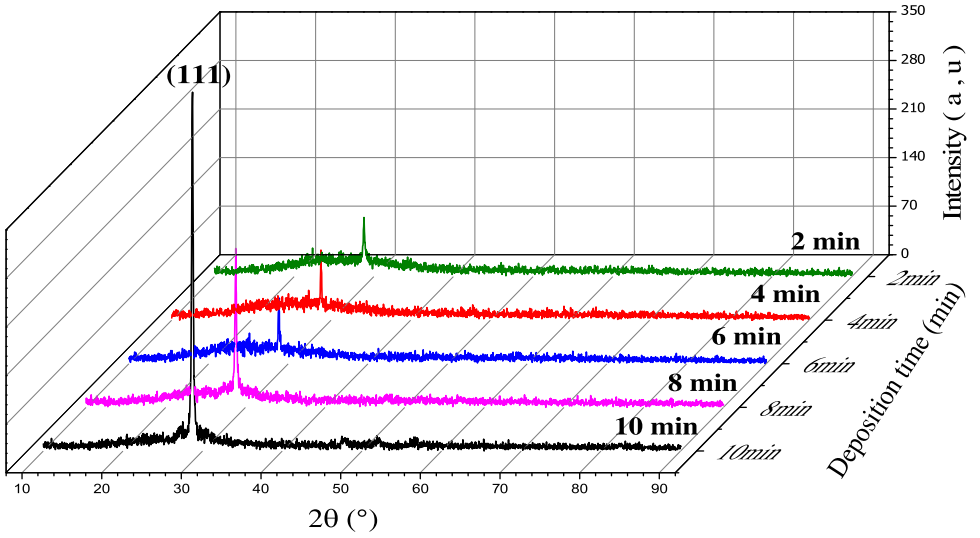

Fig. 2. XDR pattern of ZnS films deposited at various of deposition time.

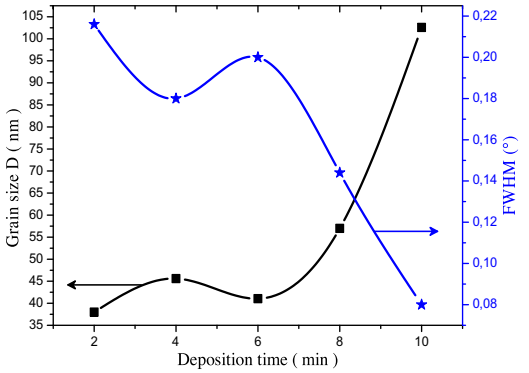

Fig. 3. Variation of grain size and FWHM of (111) peack with different deposition time.

structure (JCPDS card Nº. 55-0566) in the diffraction angle (2θ) range from 10° to 90°, which means that the planes were parallel to the substrate surface. There is no peak related to the oxidation phase (ZnO) even at the maximum deposition time, which proves that the stoichiometry of our films was improved with increasing deposition times. The same conclusion about good stoichiometry were reported by other author [15,16], for ZnS thin films obtained by spray pyrolysis at different deposition time and (Zn:S) ratio in the precursor solution (A) respectively.

Both works of Hwang et al. [17] and Ashrat et al. [18] found the same cubic phase with the preferred orientated along (111) plane of ZnS thin films prepared by RF magnetron sputtering and close-space sublimation. Fig. 2, also reveals that the intensity of (111) peak increases with the increase deposition times; it becomes narrower, intense when the deposition time equals 10 min due to the appearance of this orientation, it depends on: films and the substrate surface energies on one hand, the arriving atoms to substrate on the other hand. The growth is achieved along (111) plane due to its lowest surface energy [19]

The grain size (D) of the deposited films can be determined by using equation of Scherer [20]:

$$D = \frac{K\lambda}{\beta \cos\theta} \tag{1}$$

Where K is approximately equal to 0.94, λ = 1.54184 Å, θ is the diffraction angle and β is the width of diffraction line at half maximum intensity.

The grain size results are presented in Fig. 3. It can be observed there is a slight increase with increasing in deposition times between 2 and 6 min (38–57 nm) and this result is in good agreement with the reported ones by others authors (25–60 nm) [21], because grain size enhancement yields to the films optical transmission improvement. The solute atoms coming to the substrate surface can be diffused along the substrate surface and form clusters (nuclei) which can contribute to the formation of crystallites. At low deposition time (2–6 min), the diffusion of solute atoms on substrate surface is not

Table 2
Structural parameters of ZnS thin films at different deposition time.

Deposition time (min)	(hkl)	2θ (degree)	FWHM (degree)	D (nm)	δ x 10^{14} (Lines/m^2)	ε x 10^{-4}
2	(111)	28.7488	0.216	38	6.93	9.13
4	(111)	28.7358	0.18	45.6	4.81	7.6
6	(111)	28.806	0.2	41	5.94	8.45
8	(111)	28.7785	0.144	57	3.08	6.08
10	(111)	28.6966	0.08	102	0.95	3.38

eminent which reduced the clusters formation. Hence the density of nucleation center is small, and this lead to smaller grain size.

Then significant increases between 6 and 10 min in the crystallite size from 38 to 102 nm. Similar results have been observed by Abdi et al. [22] and Touatia et al. [23], finding that the grain size was varied between 64 and 104 nm and 50–125 nm by electron beam deposition and Vacuum Evaporation Method. With increasing the deposition time (6–10 min) the number of solute atoms arriving onto the substrate surface is increasing. Consequently the number of nuclei center formed on the substrate surface is large which leads to larger grains formation [24].

The increase of the crystallite size with the increase of deposition time may be also due to decreasing the value of full width half maximum (FWHM) corresponding to (111) peak (as seen in Fig. 3), resulting from the increasing films thickness.

A dislocation is known as a crystallographic defect, or irregularity, in a crystal structure, and its presence inside the crystallite structure strongly affects many of the properties of materials. Using the values of grain size, the dislocation density (δ), is defined as the number of dislocation lines per unit volume of the crystal, and it has been calculated depending on the Williamson and Smallman's relationship [25]:

$$\delta = \frac{1}{D^2} \tag{2}$$

The micro strains (ε) of films were estimated using the equations [26]:

$$\varepsilon = \frac{\beta \cos\theta}{4} \tag{3}$$

The structural parameters were characterized according to the calculated values of average grain size (D), micro strains (ε) and dislocation densities (δ) for ZnS thin films with different deposition time represented in Table 2

The Table 2 shows the calculated micro strain and dislocation density along the orientation (1 1 1) crystallographic plane for different deposition times. It can be seen that the maximum value of dislocation density was obtained for film sprayed at 2 min of the deposition time, the reason is due to inverse correlation between dislocation density and the grain size as confirmed in Eq. (2). As seen in the Table 2 the increase in grain size in Zinc sulphide thin films leds to a decrease in grain boundaries and it decreased dislocation defect inside the crystal lattice of the samples and the result of all this was the stress reduced in crystal structure, this later is the results of internal strains. Rahul et al. [27] have reported increases the grain size between 36.12–43.82 nm and dislocation density decreases between $7.6 \times 10^{14} - 5.2 \times 10^{14}$ line/m^2 for ZnS thin films by thermal evaporation technique.

3.2. Optical properties

The thickness of the films was calculated by weighting difference method using a sensitive microbalance according to relation (Eq. (4)):

$$thickness\,(t) = \frac{m}{\rho \times a} \tag{4}$$

Where m = mass of the deposited film, ρ = density of ZnS, equal 4.1 g/cm^3 for bulk ZnS cubic structure and a = area of film [28].

The growth rate is estimated by division thickness films on the time of deposition. The variations of the film thickness and growth rate as a function of deposition time are represented in Fig. 4. It can be observed in Fig. 4 that the film thickness and the growth rate are changing almost linearly with deposition time. The film growth is controlled by kinetics [29] of the reaction between the hot surface substrate and the amount of solution. When the deposition time increases, the mass transfer to the substrate surface increases as well and that means the increasing the mobility of the droplets reaching the substrate surface at high temperature (450° C) and increasing the number of ionized particles. Therefore, this is due to the increases of both; the reaction speeds and the kinetics of the reaction between the substrate surface and the quantity of droplets sprayed onto substrate surface and because of that it increases the growth rate which increases the thickness of ZnS thin films. The same increasing in films thickness have been reported by other authors [15,16] at deposition time between 10 and 25 min. While in deposition time equal to 10 min, we have noticed a decrease in the growth rate. This indicates that the deposited films becomes approximately in saturation case with increasing the deposition times and this is not allowed

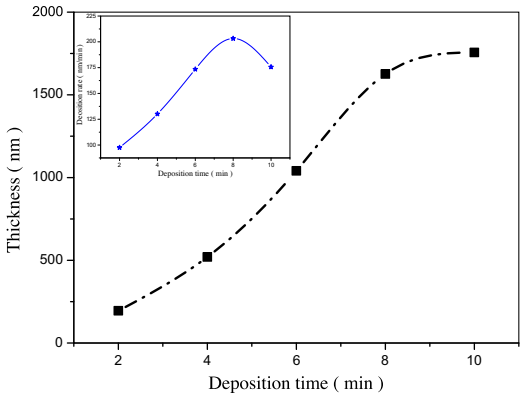

Fig. 4. Film thickness and growth rate as a function of deposition time.

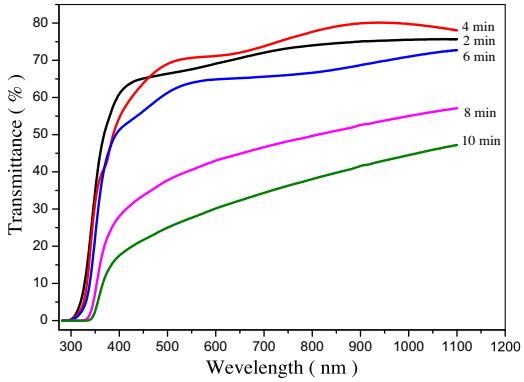

Fig. 5. Transmission of ZnS films deposited at various deposition times.

to incoming species on surface substrate which have enough appropriate places to forms more materials, which cause the decrease of the growth rate.

The high transmittance of the films in the visible range is very important for optical applications. The Fig. 5, shows the optical transmittance of ZnS films deposited at different deposition times, for incident light at wavelengths from 300 to 1100 nm.

The whole of the spectra of transmission obtained in our samples are composed of two regions: a region of strong absorption ($\lambda < 400$ nm), corresponding to fundamental absorption in thin films of ZnS. This absorption is due to the electronic transition inter band (the valence band and the band of conduction). The variation of the transmission in this region is exploited for the determination of the optical band gap energy and the disorder. It was also observed that deposition time has affected the position of absorption edge which shifted slightly to longer wavelength.

The second region of strong transparency ($\lambda > 400$ nm): the value of the transmission is about 35% to 75%, in the wavelength range of 400–800 nm. This changing in transmission values is in good agreement with that obtained values (40–70%) by Daranfed et al. [30] on ZnS thin films prepared by ultrasonic spray method. It is noticed that the transmittance decrease with the increasing deposition time, can be explained by the film thickness increase. We noticed that transmittance spectra have no interference fringe due to the incident light scattering in the material because of interface air/film roughness.

The optical band gap of ZnS films can be obtained by the absorption range in the transmittance curve and the Tauc relationship [31] (Eq. (5)):

$$\alpha h\nu = K\left(h\nu - E_g\right)^n \tag{5}$$

Where α is the absorption coefficient, K is a constant, E_g is the optical band gap and n is ½ for a direct-band gap semiconductor.

Extrapolation of the line portion of the curve to $(\alpha h\nu)^2 = 0$ gives the optical band gap. The variation of gap optic and extrapolation of the line portion of the curve to $(\alpha h\nu)^2$ as a function of $h\nu$ was shown in Fig. 6

Most of band gaps energy values are somewhat lower than that of bulk value of ZnS (3.7 eV). According to Fig. 6, the band gap energy of ZnS thin films increases first from 3.48 eV to 3.92 eV in the range 2–6 min. This result is in good agreement with that obtained by Elidrissi et al. [32], the wide band gap energy is the reason of window layer absorption decreases loses and consequently this yields to the solar cell short circuit current improvement. The increase of band gap energy is caused by film thickness increas [33] and Burnstein-Moss effect [34]. However, after that, the gap optic decreased from 3.92 eV to

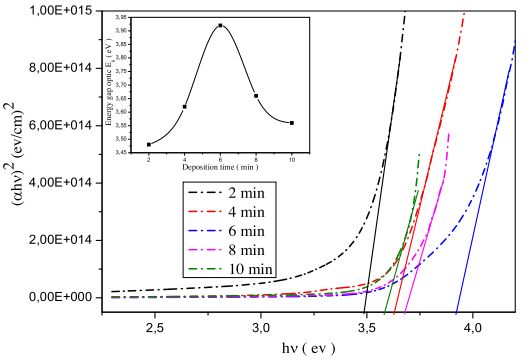

Fig. 6. Band gap energy of the ZnS films as a function of deposition time.

Table 3
Refractive index of ZnS thin film at different deposition time calculated by Herve- Vandamme equation.

Deposition time (min)	Band gap E_g (eV)	Crystallite size D (nm)	Refractive index n
2	3.48	38	2.21
4	3.62	45.6	2.18
6	3.92	41	2.11
8	3.66	57	2.17
10	3.56	102	2.19

3.56 eV with the increasing deposition time, it can be explained this decrease in the gap optic energy to quantum size effect [35] owing to increased crystallite size. Similar results have been observed by Abduljabbar (3.7–3.3 eV) [36], Yildrim et al. (3.73–3.57 eV)[37] and Nadeem et al. (3.84–3.51 eV)[38].

The refractive index (n) of ZnS thin films elaborated at different deposition time is calculated using the model of Herve-Vandamme. The Herve- Vandamme relationship [39] is:

$$n^2 = 1 + \left(\frac{A}{E_g + B}\right)^2 \tag{6}$$

Where A and B are constants as A ≈ 13.6 eV and B ≈ 3.4 eV and E_g is the experimental values of gap optic energy.

The refractive index of ZnS thin films elaborated at different values of deposition time is illustrated in Table 3.

As observed in Table 3 the refractive index decreases between 2.11 and 2.21 in the range 2–6 min, then increased with the increase the deposition time. Abduljabbar [40] had reported in earlier work, the value of the refractive index of ZnS thin films was around 2.13–2.19 at room temperature and at different temperatures (200 °C, 300 °C and 400 °C). We can attribute this decrease as follows: the increase of the grain size due to decrease of grains boundaries, this may be due to reduced of the stress in the crystalline network of the ZnS thin films. Younghun et al. [41] have also reported the effects of biaxial stress on the refractive index of ZnO:Ga, so they have found that the refractive index decreases with increasing biaxial tensile stress.

3.3. Electrical properties

For our study the resistivity is calculated by the following equation [42]:

$$\rho = Rd \tag{7}$$

Where ρ is the resistivity, R is the square resistance and d the sample thickness. The variations of ZnS layers resistivity and conductivity versus the deposition time are presented in Fig. 7.

It could be observed that the resistivity of the grown films increases from $1.51 \times 10^5\ \Omega$ cm to $20.84 \times 10^5\ \Omega$ cm with the increasing of the deposition time. These results are lower than Turan et al. ones [43], who studied the electrical properties of ZnO/Au/ZnS/Au films deposited by ultrasonic spray pyrolysis. Hence, the grain size enlargement leads to a decrease in grain boundary effects, because the boundary hinders the conduction mechanism of carriers charge, and this is the reason for an increase in resistivity.

As observed that the increase in the thickness of the samples led also to the increase of the resistivity of ZnS thin films as showing in Eq. (7). Therefore, the resistivity was affected by carrier concentration and deposition time.

4. Conclusion

In this work, we have been shown that the deposition time plays a fundamental role on the properties of ZnS thin films deposited by ultrasonic spray on to glass at 450 °C substrate temperature. The XRD measurements reveal that the films

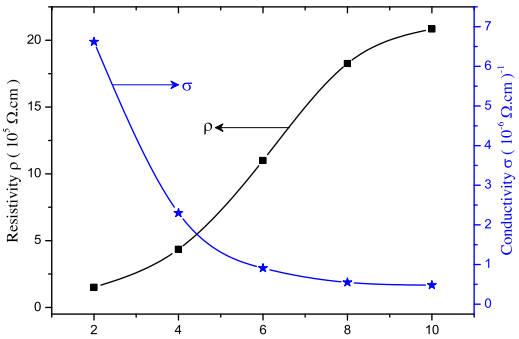

Fig. 7. Variation of the resistivity and conductivity of ZnS thin films with different deposition time.

deposited at 10 min have a strongly (111) preferred orientation and are parallel to the substrate surface. The smallest FWHM value of 0.08° has been also been observed for these films, indicating that the crystallinity of the films can be improved by increasing the deposition time. The grain sizes of ZnS calculated by Scherer relationship were found between 38 and 102 nm. It has been found that the transmittance decreases with the increase of deposition time. The calculated band gap energy of ZnS has given the values in the range of 3.48–3.92 eV. Furthermore, the electrical resistivity (ρ) increased when the deposition time increases.

It can be concluded that the perfect condition for the best application photovoltaic cell efficiency of ZnS thin films is to increase the deposition time, owing to band gap energy widening, which can be used as a window layer in heterojunction photovoltaic solar cell or can be used as a reflector and dielectric filter because of its high refractive index (2.2) and its high transmittance in the visible range

References

[1] Zhong Chen, Sheng Zhou, Yang Li, Xiao Xia Li, Yangsheng Li, Wei Sun, Guihua Liu, Nan Chen, Guoping Dua, Strong blue luminescence of O^{2-}-doped ZnS nanoparticles synthesized by a low temperature solid state reaction method, Mater. Sci. Semicond. Process. 16 (2013) 833–837.
[2] Abdelhak Jrad, Wafa Naffouti, Tarek Ben Nasr, Najoua Turki-Kamoun, Comprehensive optical studies on Ga-doped ZnS thin films synthesized by chemical bath deposition, J. Lumin. 173 (2016) 135–140.
[3] Yu-hong Huang, Wan-qi Jie, Yan Zhou, Gang-qiang Zha, Structural stability, band structure and magnetic properties of ZnS and $Zn_{0.75}Cr_{0.25}S$ under pressure, J. Alloys Compd. 549 (2013) 184–189.
[4] E. Mastio, E. Fogarassy, W. Cranton, C. Thomas, Ablation study on pulsed KrF laser annealed electroluminescent ZnS:Mn/Y_2O_3 multilayers deposited on Si, Appl. Surf. Sci. 154 (2000) 35–39.
[5] D. Denzler, M. Olschewski, K. Sattler, Luminescence studies of localized gap states in colloidal ZnS nanocrystals, J. Appl. Phys. 84 (1998) 2841–2845.
[6] D.R. Acosta, E.P. Zironi, E. Montoya, W. Estrada, About the structural, optical and electrical properties of SnO_2 films produced by spray pyrolysis from solutions with low and high contents of fluorine, Thin Solid Films 288 (1996) 1–7.
[7] D. Gal, G. Hodes, D. Lincot, H.W. Schock, Electrochemical deposition of zinc oxide films from non-aqueous solution: a new buffer/window process for thin film solar cells, Thin Solid Films 361-362 (2000) 79–83.
[8] S. Yano, R. Schroeder, B. Ullrich, H. Sakai, Absorption and photocurrent properties of thin ZnS films formed by pulsed-laser deposition on quartz, Thin Solid Films 423 (2003) 273–276.
[9] D. Barreca, G. Bruno, A. Gasparotto, M. Losurdo, E. Tondello, Nanostructure and optical properties of CeO_2 thin films obtained by plasma-enhanced chemical vapor deposition, Mater. Sci. Eng. 23 (2003) 1013–1016.
[10] Y. Kavanagh, D.C. Cameron, Zinc sulfide thin films produced by sulfidation of sol-gel deposited zinc oxide, Thin Solid Films 398-399 (2001) 24–28.
[11] M.A. Hernandez-Fenollosa, M.C. Lopez, V. Donderis, M. Gonzalez, B. Mari, J.R. Ramos-Barrado, Role of precursors on morphology and optical properties of ZnS thin films prepared by chemical spray pyrolysis, Thin Solid Films 516 (2008) 1622–1625.
[12] Jenifar Sultana, Somdatta Paul, Anupam Karmakar, Ren Yi, Goutam Kumar Dalapati, Sanatan Chattopadhyay, Chemical bath deposited (CBD) CuO thin films on n-silicon substrate for electronic and optical applications: impact of growth time, Appl. Surf. Sci. 418 (2017) 380–387.
[13] M.J. Alam, D.C. Cameron, Investigation of annealing effects on sol–gel deposited indium tin oxide thin films in different atmospheres, Thin Solid Films 420–421 (2002) 76–82.
[14] H. Cachet, J. Bruneaux, G. Folcher, C. Leí vy-Cleíment, C. Vard, M. Neumann Spallart, n-Si/SnO_2 junctions based on macroporous silicon for photoconversion, Sol. Energy Mater. Sol. Cells 46 (1997) 101–114.
[15] H.H. Afifi, S.A. Mahmoud, A. Ashour, Structural study of ZnS thin films prepared by spray pyrolysis, Thin Solid Films 263 (1995) 248–251.
[16] M.C. Lopez, J.P. Espinos, F. Martın, D. Leinen, J.R. Ramos-Barrado, Growth of ZnS thin films obtained by chemical spray pyrolysis: the influence of precursors, J. Cryst. Growth 285 (2005) 66–75.
[17] Dong Hyun Hwang, Jung Hoon Ahn, Kwun Nam Hui, Kwan San Hui, Young Guk Son, Structural and optical properties of ZnS thin films deposited by RF magnetron sputtering, Nanoscale Res. Lett. 7 (2012) 26.
[18] M. Ashrat, M. Mehmood, A. Qayyum, Influence of source-to-substrate distance on the properties of ZnS films grown by close-space sublimation, Semiconductors 46 (10) (2012) 1326–1330, ISSN 1063–7826.
[19] K. Wright, G.W. Watson, S.C. Parker, D.J. Vaughan, Simulation of the structure and stability of sphalerite (ZnS) surfaces, Am. Mineral. 83 (1998) 141–146.
[20] M. Nada Saeed, Structural and optical properties of ZnS thin films prepared by spray pyrolysis technique, J. Al-Nahrain Univ. Vol.14 (June (2)) (2011) 86–92.
[21] A. Djelloul, M. Adnane, Y. Larbah, T. Sahraoui, C. Zegadi, A. Maha, B. Rahal, Properties study of ZnS thin films prepared by spray pyrolysis method, J. Nano- Electron. Phys. 7 (2015) 04045 (5pp).
[22] Fatemeh Abdi, Hadi Savaloni, Investigation of the growth conditions on the nano-structure and electrical properties of ZnS chiral sculptured thin films, Appl. Surf. Sci. 330 (2015) 74–84.
[23] R. Touati, M. Ben Rabeh, M. Kanzari, Structural and optical properties of the new absorber Cu_2ZnSnS_4 thin films grown by vacuum evaporation method, Energy Procedia 44 (2014) 44–51.

[24] Kirill Bordo, Horst-Günter Rubahn, Effect of deposition rate on structure and surface morphology of thin evaporated Al films on dielectrics and semiconductors, Mater. Sci. (Medziagotyra) 18 (4) (2012) 313–317, ISSN 1392–1320.
[25] B. Kherchachi, A. Attaf, H. Saidi, A. Bouhdjer, H. Bendjedidi, Y. Benkhetta, R. Azizi, Structural, optical and electrical properties of SnxSy thin films grown by spray ultrasonic, J. Semicond. 37 (2) (2016).
[26] C.K. De, N.K. Misra, X-ray diffraction analysis of lattice defects of ZnSe thin films deposited at different substrate temperatures, Indian J. Phys. A 71 (535) (1997).
[27] Rahul Vishwakarma, Effect of substrate temperature on ZnS films prepared by thermal evaporation technique, J. Theor. Appl. Phys. (2015), http://dx.doi.org/10.1007/s40094-015-0177-5.
[28] Jyoti P Borah, J. Barman, K.C. Sarma, Structural and optical properties of ZnS nanoparticles, Chalcogenide Lett. Vol. 5 (September (9)) (2008) 201–208.
[29] J.M. Blocher, Coating of glass by chemical vapor deposition, Thin Solid Films 77 (1981) 51–64.
[30] W. Daranfed, M.S. Aida, A. Hafdallah, H. Lekiket, Substrate temperature influence on ZnS thin films prepared by ultrasonic spray, Thin Solid Films 518 (2009) 1082–1084.
[31] C. Mehta, G.S.S. Saini, J.M. Abbas, S.K. Tripathi, Effect of deposition parameters on structural, optical and electrical properties of nanocrystalline ZnSe thin films, Appl. Surf. Sci. 256 (2009) 608–614.
[32] B. Elidrissi, M. Addou, M. Regragui, A. Bougrine, A. Kachouane, J.C. Bernède, Structure, composition and optical properties of ZnS thin films prepared by spray pyrolysis, Mater. Chem. Phys. 68 (2001) 175–179.
[33] Cleva W. Ow-Yang, Hyo-young Yeom, David C. Paine, Fabrication of transparent conducting amorphous Zn–Sn–In–O thin films by direct current magnetron sputtering, Thin Solid Films 516 (2008) 3105–3111.
[34] R. Ayouchi, D. Leinen, F. Martin, M. Gabas, E. Dalchiele, J.R. Ramos-Barrado, Preparation and characterization of transparent ZnO thin films obtained by spray pyrolysis, Thin Solid Films 426 (2003) 68–77.
[35] N. Bouguila, D. Bchiri, M. Kraini, A. Timoumi, I. Halidou, K. Khirouni, S. Alaya, Structural, morphological and optical properties of annealed ZnS thin films deposited by spray technique, J. Mater. Sci. Mater. Electron. (2015), http://dx.doi.org/10.1007/s10854-015-3659-y.
[36] Layth M. Abduljabbar, Study the effect of annealing on optical and electrical properties of ZnS thin film prepared by CO_2 laser deposition technique, Iraqi J. Laser Part 13 (2014) 29–35.
[37] A. Ates, M.A. Yıldırım, M. Kundakcı, A. Astam, Annealing and light effect on optical and electrical properties of ZnS thin films grown with the SILAR method, Mater. Sci. Semicond. Process. 10 (2007) 281–286.
[38] M. Nadeem, W. Ahmed, Optical properties of ZnS thin films, Turk. J. Phys. 24 (2000) 651–659.
[39] M. Mekhnache, A. Drici, L. Saad Hamideche, H. Benzarouk, A. Amara, L. Cattin, J.C. Bernede, M. Guerioune, Properties of ZnO thin films deposited on (glass, ITO and ZnO:Al) substrates, Superlattices Microstruct. 49 (2011) 510–518.
[40] Layth M. Abduljabbar, Study the effect of annealing on optical and electrical properties of ZnS thin film prepared by CO_2 laser deposition technique, Iraqi J. Laser 13 (2014) 29–35.
[41] Younghun Hwang, Heejin Ahn, Manil Kang, Youngho Uma, Hyoyeol Park, Electronic and optical properties in ZnO:Ga thin films induced by substrate stress, J. Phys. Chem. Solids 87 (2015) 122–127.
[42] Z. Ben Achour, T. Ktari, B. Ouertani, O. Touayar, B. Bessais, J. Ben Brahim, Effect of doping level and spray time on zinc oxide thin films produced by spray pyrolysis for transparent electrodes applications, Sens. Actuators A 134 (2007) 447–451.
[43] Evren Turan, Muhsin Zor, A. Senol Aybek, Metin Kul, Electrical properties of ZnO/Au/ZnS/Au films deposited by ultrasonic spray pyrolysis, Thin Solid Films 515 (2007) 8752–8755.